Diffusion in Deterministic Interacting Lattice Systems

Marko Medenjak, Katja Klobas, and Tomaž Prosen
Faculty of Mathematics and Physics, University of Ljubljana, Jadranska 19, SI-1000 Ljubljana, Slovenia
(Received 17 May 2017; revised manuscript received 19 July 2017; published 14 September 2017)

We study reversible deterministic dynamics of classical charged particles on a lattice with hard-core interaction. It is rigorously shown that the system exhibits three types of transport phenomena, ranging from ballistic, through diffusive to insulating. By obtaining an exact expressions for the current time-autocorrelation function we are able to calculate the linear response transport coefficients, such as the diffusion constant and the Drude weight. Additionally, we calculate the long-time charge profile after an inhomogeneous quench and obtain diffusive profilewith the Green-Kubo diffusion constant. Exact analytical results are corroborated by Monte Carlo simulations.

DOI: 10.1103/PhysRevLett.119.110603

Introduction.—Understanding out-of-equilibrium phenomena has been at the forefront of condensed matter physics of the last decade. Despite the efforts, we have only recently gained a considerable insight into the microscopic origins of the transport in interacting systems in terms of an emerging field of generalized hydrodynamics (GHD) [1–11]. While GHD provides a general framework to analytically deal with the ballistic transport, in particular, in integrable systems, it lacks an extension which would enable us to study normal, diffusive transport. In this regard, there are only a few results on lower bounding the diffusion constant [12,13].

Since the integrable systems are characterized by ballistically propagating excitations [14], the question of how the diffusion, which is usually related to microscopic chaos, arises in integrable, locally interacting, clean and deterministic (i.e., nondisordered and nondissipative) systems is puzzling to say the least [15–20]. A great deal of attention has been devoted to the study of inhomogeneous quench problems, where two chains in equilibrium with distinct temperatures or chemical potentials are joined together and then let to evolve under a homogeneous Hamiltonian [1–9,21]. In such situations, nonequilibrium steady states typically emerge on ballistic lines $x = vt$. However, for systems exhibiting paritylike symmetries, with respect to which the initial quench state is symmetric and the current antisymmetric, the ballistic transport channel may close and time-dependent density matrix renormalization group simulations clearly indicate that the steady state arises along the diffusive lines $x = \xi\sqrt{t}$ [15].

In this Letter we expound one possible general mechanism for diffusive behavior in interacting systems, which as we show on an example, is connected to the interplay between freely propagating neutral degrees of freedom and insulating behavior of charge carrying ones. The model in question is a simple, reversible cellular automaton, consisting of three types of particles: freely moving vacancies, and hard-core interacting positive and negative charges. Similar automata provide caricatures of mechanical laws of motion and were studied in the context of integrability [22–25]. Despite the integrability, obtaining the full time dependence is usually intractable, rendering the calculation of transport coefficients inaccessible. In our model, however, we explicitly compute the time dependence of current time autocorrelation functions in separable equilibrium states, and solve the inhomogeneous quench problem with arbitrary initial charge density bias resulting in a universal diffusive error function scaling profile. Depending on the density of vacancies and the imbalance of positive and negative charge three different regimes are identified. The absence of vacancies renders the system insulating, while in a generic case of the charge imbalance the system exhibits ideal transport. In the regime with a finite density of vacancies and without the charge imbalance, including the maximum entropy state, the model exhibits purely diffusive transport.

The model.—Consider a deterministic, reversible cellular automaton defined on the chain with an even length of n sites. Each site can be either vacant (state $\emptyset$), or occupied by a positively or negatively charged particle (state $+$ or $-$). The dynamics of the lattice configuration, $\underline{s} = (s_1, \ldots, s_n)$, $s_x \in \{\emptyset, +, -\}$, can be expressed in terms of a local two site mapping $\phi_{x,x+1}(\underline{s}) = (s_1, s_2, \ldots, s'_x, s'_{x+1}, \ldots, s_n)$, where the updated elements (s'_x, s'_{x+1}) are obtained from the initial ones (s_x, s_{x+1}), by a self-inverse transformation

$$(\emptyset,\emptyset) \leftrightarrow (\emptyset,\emptyset), \quad (\emptyset,\alpha) \leftrightarrow (\alpha,\emptyset), \quad (\alpha,\beta) \leftrightarrow (\alpha,\beta), \qquad (1)$$

with $\alpha, \beta \in \{+, -\}$. The local process describes the elastic scattering of charged particles. The lattice configuration at time t, $\underline{s}^t = \phi(\underline{s}^{t-1})$, can be expressed in terms of a two step propagator $\phi = \phi^o \circ \phi^e$ given by sequences of disjoint local mappings [Relation (1)] $\phi^o = \phi_{1,2} \circ \ldots \circ \phi_{n-1,n}$, $\phi^e = \phi_{2,3} \circ \ldots \circ \phi_{n,1}$, intertwining odd-even and even-odd sites, respectively. The dynamics of charges is induced by freely propagating vacancies, while the clustered particles remain frozen in time as illustrated in Fig. 1. The cellular automaton

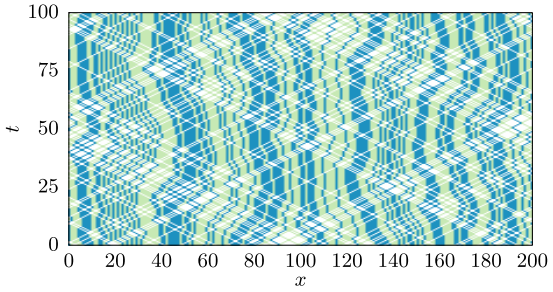

FIG. 1. Time evolution of a random maximum entropy configuration ($\rho = 2/3$, $\mu = 0$) for 200 sites. Particles $+$, $-$, and vacancies $\emptyset$ are in blue, green, and white, respectively.

admits a mechanical analogy in terms of a two-species, synchronous hard-point gas if particles at occupied sites x are attributed velocities $2(-1)^x$ or $-2(-1)^x$, at odd or even steps, corresponding, respectively, to integer or half-integer times [26].

We are interested in the dynamics of the charge $q_x^t = s_x^t + s_{x+1}^t$ corresponding to sites x and $x+1$ at time t, with $s_x^t = \pm 1$, if the site x is occupied by the positive or negative charge, and $s_x^t = 0$ otherwise. The total charge $Q^t = \sum_x q_x^t$, is a constant of motion. The corresponding current $J^t = \sum_x j_x^t$ can be defined on the intermediate time steps (see Fig. 2) as

$$j_x^{t+1/2} = 2(-1)^x (s_x^{t+1/2} - s_{x+1}^{t+1/2})(s_x^{t+1/2} + s_{x+1}^{t+1/2})^2, \qquad (2)$$

where j_x denotes the local density. The omitted superscript corresponds to time $t = 0$. One can check that the continuity equation holds:

$$q_x^{t+1} - q_x^t + \frac{1}{2}(j_{x+1}^{t+1/2} - j_{x-1}^{t+1/2}) = 0. \qquad (3)$$

To carry out the calculations we introduce a multiplicative algebra $\mathcal{A}$ of observables—functions over the configuration space with a *local* basis

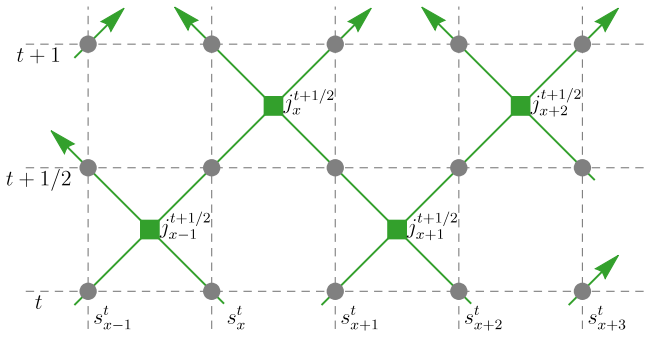

FIG. 2. Scheme of the model: Gray disks denote the sites to which the particles or vacancies (s_x^t) are assigned, and green boxes where the particles scatter carry the local current. The particles can be imagined to move along green lines. Pairs $(x-1, x)$, $(x+1, x+2)$, …, are updated between time slices t and $t + \frac{1}{2}$, while the shifted pairs are updated in the following half-time step.

$$[\alpha]_x(\underline{s}) = \delta_{\alpha_x, s_x}, \qquad \alpha \in \{\emptyset, +, -\}, \qquad (4)$$

$$[\alpha_1 \alpha_2 \ldots \alpha_r]_x = [\alpha_1]_x [\alpha_2]_{x+1} \cdots [\alpha_r]_{x+r-1}. \qquad (5)$$

The position x will be dropped when clear from the context. The dynamics of observables $a^t(\underline{s}) \equiv U^t a(\underline{s}) = a(\phi^t(\underline{s}))$ is given by a $3^n \times 3^n$ matrix U [32] factorized as

$$U = U^o U^e, \quad U^o = \prod_{x=1}^{n/2} U_{2x-1,2x}, \quad U^e = \prod_{x=1}^{n/2} U_{2x,2x+1}. \qquad (6)$$

Note that the local propagator obeys Yang-Baxter equation $U_{x,y} U_{y,z} U_{x,y} = U_{y,z} U_{x,y} U_{y,z}$. We define the unnormalized maximum entropy state $\langle a \rangle = \sum_{\underline{s}} a(\underline{s})$ in terms of which an expectation value in any probability distribution (state) p can be expressed as $\langle a \rangle_p = \langle ap \rangle$. We introduce an alternative local basis and its dual

$$\begin{aligned}
&[0] = [\emptyset] + [+] + [-], && [0]' = (1-\rho)[\emptyset] + \frac{\rho}{2}([+] + [-]), \\
&[1] = [+] - [-], && [1]' = \frac{1}{2}([+] - [-]), \\
&[2] = \frac{1}{1-\rho}[\emptyset] - [0], && [2]' = \frac{1-\rho}{2}(2[\emptyset] - [+] - [-]),
\end{aligned} \qquad (7)$$

$\langle [\alpha][\beta]' \rangle = \delta_{\alpha,\beta}$, $\alpha, \beta \in \{0, 1, 2\}$. This basis has the following properties: $[0] \equiv 1$ (identity in $\mathcal{A}$), $[1]$ corresponds to the imbalance of charge, and $\langle [2] \rangle_p = 0$ for the class of probability distributions p introduced below, with the particle density ρ. These properties enable us to study the dynamics on the reduced space. The local charge and current now read

$$q_x = [10]_x + [01]_x, \qquad (8)$$

$$j_x = 2(1-\rho)(-1)^x ([10]_x - [01]_x + [12]_x - [21]_x). \qquad (9)$$

Linear response.—According to Einstein's relation the diffusion coefficient $\mathcal{D}$ is connected to Green-Kubo conductivity (Sec. A of the Supplemental Material [33])

$$\sigma = \frac{1}{2} C(0) + \sum_{t=1}^{\infty} C(t), \qquad (10)$$

as $\sigma = \chi \mathcal{D}$, χ being the static susceptibility (the second moment of charge Q). $C(t) = \lim_{n\to\infty} (1/n) \langle J U^t J \rangle_p$ is the current correlation function, with p being an equilibrium state, $Up = p$, and n the system size. Another important transport coefficient, corresponding to the rate at which the conductivity diverges [34], is the Drude weight, $D = C(\infty)$. In case of nonvanishing Drude weight, the diffusion constant can be regularized by subtracting the ballistic contribution from the correlator $C(t) \to C(t) - C(\infty)$ [1,35].

We restrict the discussion to translationally invariant product equilibrium states $p = p(\rho,\mu) = \prod_{x=1}^{n} p_x$,

$$p_x = [0]'_x + \mu[1]'_x, \qquad 0 \le \rho \le 1, \qquad -\rho \le \mu \le \rho. \quad (11)$$

Note that $[0]'_x$ depends on ρ. The density ρ represents the probability of a lattice site being occupied by a charged particle, while the chemical potential μ corresponds to the charge imbalance. The static susceptibility in such a state is $\chi = 4(\rho - \mu^2)$.

Diffusive regime.—Initially we consider a balanced equilibrium state with $\mu = 0$ and arbitrary ρ for which the following orthogonality relations hold,

$$\langle [0][1] \rangle_p = \langle [0][2] \rangle_p = \langle [1][2] \rangle_p = 0. \quad (12)$$

As a consequence only the observables with a single occurrence of [1] and at most one [2] in the propagated current J^t can contribute to the expectation value (10). The local observables that are relevant for the calculation of the diffusion constant are $y_0 = \sum_x ([10]_{2x} - [01]_{2x})$, $y_1 = \sum_x ([12]_{2x} - [21]_{2x})$, and $y_2 = \sum_x ([012]_{2x} - [021]_{2x})$, in terms of which the current reads $J = 2(1-\rho) \times (-2y_0 - y_1 + y_2)$. In addition, we note that the two steps of the propagator are conjugated $U^o = S^{-1}U^eS$ by a lattice shift, defined as $S[\underline{\alpha}]_x = [\underline{\alpha}]_{x+1}$. Since y_α are translationally invariant, i.e., $S^2 y_\alpha = y_\alpha$, the complete propagator on the relevant subspace reads $U = (SU^e)^2$. Under the half-time propagation SU^e the observables y_0 and y_1 map into linear combinations of y_0 and y_2. Because of the ballistic propagation of [2], $U_{1,2}[02] = [20]$, $U_{1,2}[20] = [02]$, any additional basis operators appearing in y_2^t, $t > 0$, are orthogonal to J, since there is always at least one occurrence of [0] between [1] and [2]. Therefore, in order to compute $C(t)$, we only have to consider the time evolution restricted to the subspace spanned by $\{y_\alpha\}$. Half-time step propagator SU^e projected to this basis reads (see sec. B of the Supplemental Material [33] for details)

$$\mathcal{U} = \begin{bmatrix} 1-2\rho & 2\rho & 0 \\ 0 & 0 & 0 \\ -2(1-\rho) & 1-2\rho & 0 \end{bmatrix}, \quad (13)$$

and yields the following simple expression for the current-autocorrelation function

$$C(t) = 4\rho(1-\rho)[2(1-\rho),\ \rho,\ -p]\mathcal{U}^{2t}\begin{bmatrix} 2 \\ 1 \\ -1 \end{bmatrix} = \begin{cases} 8\rho(2-\rho)(1-\rho); & t = 0, \\ 16\rho(1-\rho)^4(1-2\rho)^{2t-2}; & t \ge 1. \end{cases} \quad (14)$$

The row vector contains properly normalized overlaps $\langle y_\alpha J \rangle_p$, while the column vector is proportional to the current J expressed in the basis $\{y_\alpha\}$. One can then easily calculate the conductivity and the diffusion constant

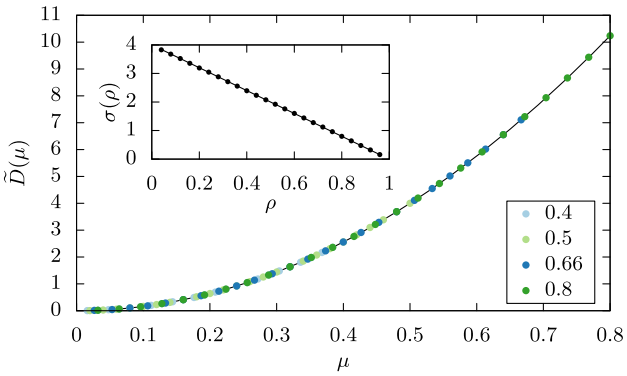

FIG. 3. The comparison between the exact and numerically estimated Drude weight $\tilde{D}$ and conductivity σ. Drude weight is rescaled as $\tilde{D} = D/(\rho^{-1} - 1)$. Points with different colors correspond to numerically calculated Drude weights at different values of ρ and black points (inset) are numerically estimated values of the conductivity (at $\mu = 0$). The black lines correspond to exact values Eqs. (15) and (18).

$$\sigma = 4(1-\rho), \qquad \mathcal{D} = \rho^{-1} - 1, \quad (15)$$

which agree with Monte Carlo simulations (see Fig. 3).

Ballistic regime.—By introducing the charge imbalance $\mu \neq 0$, the local observables cease to be orthogonal, $\langle [2][1] \rangle_{p(\rho,\mu)} \neq 0$. However, we may still consider only a subspace of observables, with at most one occurrence of [2] and a single [1]. In this case the relevant subspace is spanned by $\{y_0, y_1, z^0_{2d}, z^1_{2d+1}; d \ge 0\}$, with the observables z^k_d defined as

$$z^k_d = \sum_x ([00\ldots\underbrace{010\ldots}_{k}\underbrace{012}_{d}]_{2x} - [020\ldots\underbrace{010\ldots}_{d}\underbrace{0}_{k}]_{2x}). \quad (16)$$

Performing a similar calculation as above we obtain the following expression for the time autocorrelation function (Sec. B of the Supplemental Material [33])

$$\frac{C(t)}{8\bar{\rho}} = \begin{cases} \mu^2 + \rho(2-\rho); & t = 0, \\ \frac{2\mu^2}{\rho} + 2\bar{\rho}^3(1-2\rho)^{2t-2}(\rho - \frac{\mu^2}{\rho}); & t \ge 1, \end{cases} \quad (17)$$

with $\bar{\rho} = 1 - \rho$, which immediately yields the exact expression for the Drude weight

$$D = 16(\rho^{-1} - 1)\mu^2, \quad (18)$$

again agreeing excellently with numerics (Fig. 3). The details regarding Monte Carlo simulations are presented in Sec. D of the Supplemental Material [33].

Inhomogeneous quench.—Let us consider dynamics of charges starting from the product initial state p with uniform density ρ and two distinct chemical potentials μ_L, μ_R on the left and the right half of the chain, which can be expressed locally as

$$p_{n/2+x} = [0]' + \mu_x [1]', \tag{19}$$

with $\mu_x = \mu_L$ for $x \leq 0$ and μ_R for $x > 0$. We shall now discuss the time evolution of the centered charge profile

$$f(x,t) = \langle U^t q_{n/2+2x-1} \rangle_p = \langle q_{n/2+2x-1} \rangle_{U^{-t}p}. \tag{20}$$

In particular, we are interested in the dynamics inside of the light-cone $|x| \leq t$ with $n \geq 8t+2$, so that the boundary values of the profile are constant $f(\mp t, t) = 2\mu_{L,R}$.

Because of the conservation of the number of $\alpha_j = 1$ in the adjoint time evolution $U^{-t}p$ expressed in the dual basis $[\underline{\alpha}]'$, the initial state p can be replaced by

$$\tilde{p} = \sum_{x=-\frac{n}{2}+1}^{\frac{n}{2}} \mu_x e_x, \qquad e_x = [0 \ldots 0 \underbrace{10 \ldots}_{\frac{n}{2}+x-1} \underbrace{0]'}_{\frac{n}{2}-x}. \tag{21}$$

Here we use the dual space version of the argument used in the computation of correlation functions. After half of the time step the time propagated charge density (21) consists of the terms including a single occurrence of $[1]'$ and combinations of $[1]'$ and $[2]'$ on neighboring sites on the background of $[0 \ldots 0]'$. Using the argument of the freely propagating $[2]'$, namely, $U_{1,2}[02]' = [20]'$, $U_{1,2}[20]' = [02]'$, we can conclude that the terms containing $[2]'$ can be disregarded at all time steps due to the orthogonality to charge densities q_x. The complete time propagation on the relevant subspace, spanned by $\{e_x\}$, is described by a cyclic block three-diagonal matrix

$$\mathcal{U} = \begin{bmatrix} \ddots & \ddots & \ddots & & & & \\ & c & a & b & & & \\ & & c & a & b & & \\ & & & \ddots & \ddots & \ddots & \end{bmatrix}, \tag{22}$$

where a, b, c are 2×2 blocks. The projected initial state (21) reads $\underline{p} = \bigoplus_{x=1}^{n} \mu_{x-n/2}$. Assuming that $n \geq 8t+2$, the charge profile (20) inside of the light cone no longer depends on n. Thus, the limit $n \to \infty$ can be applied and an infinite matrix $\mathcal{U}$ can be diagonalized using the block Fourier transform, yielding two bands of eigenvalues $\lambda_{1,2}(k)$, $k \in [-\pi, \pi]$ and Bloch eigenvectors $\underline{\omega}_{1,2}(k) = \bigoplus_{x \in \mathbb{Z}} \underline{v}_{1,2}(k) e^{ikx}$ (see Sec. C of the Supplemental Material [33] for details). Additionally, note that $\langle q_x U^{-t} e_y \rangle = 0$, if $|x-y| > 2t$, so the charge density profile can finally be expressed as a Fourier integral

$$f(x,t) = \sum_{y=x-t}^{x+t} \mu_{2y} \int_{-\pi}^{\pi} dk e^{ik(x-y)} \sum_{j=1}^{2} \lambda_j(k)^t \tilde{\alpha}_j(k), \tag{23}$$

where $\tilde{\alpha}_{1,2}(k) = \alpha_{1,2}(k)([1,1] \cdot \underline{v}_{1,2}(k))$, and $\alpha_{1,2}(k)$ are the coefficients expressing the vector [1, 1] in terms of Bloch vectors $v_{1,2}(k)$ (details in Sec. C of the Supplemental Material [33]). We are interested in the behavior of $f(x,t)$ on the diffusive lines $2x = \xi\sqrt{t}$ in the large time limit $\tilde{f}(\xi) = \lim_{t\to\infty} f(\xi\sqrt{t}/2, t)$. In this limit, the contribution from the term proportional to $\lambda_2(k)^t$ can be disregarded, since $\sup_k |\lambda_2(k)| < 1$. Additionally, one should note that $\lambda_1(0) = 1$, therefore the large t asymptotics of Eq. (23) can be obtained by expanding $\lambda_1(k)$ around $k = 0$, $\lambda_1(k)^t \simeq e^{-\gamma k^2 t}$, $\gamma = (1-\rho)/4\rho$. Introducing a new variable $h = k\sqrt{t}$ the integral (23) can be calculated exactly in the scaling limit $x, t \to \infty$ with $x/\sqrt{t}$ fixed, yielding

$$\tilde{f}(\xi) = (\mu_R + \mu_L) + (\mu_R - \mu_L) \mathrm{erf}\left(\frac{\xi}{4\sqrt{\gamma}}\right). \tag{24}$$

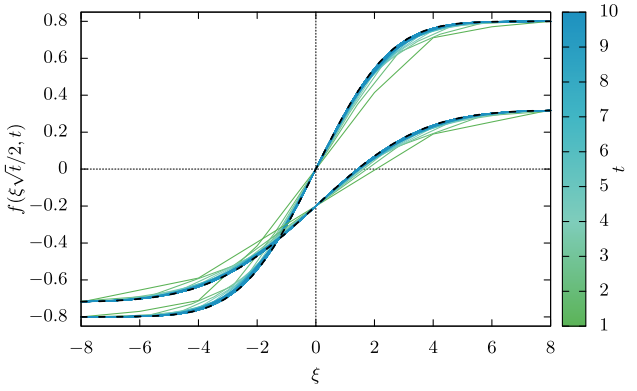

FIG. 4. Charge profiles $f(\xi\sqrt{t}/2, t)$ after the inhomogeneous quench. Curves with different colors correspond to different times t. The profiles converge to the estimated asymptotic profiles (dashed lines) given by Eq. (24). The parameters (ρ, μ_L, μ_R) are $(1/2, -0.36, 0.16)$ and $(2/3, -0.4, 0.4)$.

The agreement between the exact and numerical result can be seen in Fig. 4. Since the solution of the diffusion equation $(\partial/\partial t) f(x,t) = \mathcal{D}(\partial^2/\partial x^2) f(x,t)$ for a step initial data reads $f(x,t) \sim \mathrm{erf}(x/\sqrt{4\mathcal{D}t})$, the diffusion constant is $\mathcal{D} = 4\gamma = \rho^{-1} - 1$.

Contrary to the linear response, the inhomogeneous quench does not excite any ballistic transport for the specific class of initial states considered [Eq. (19)] even for $\mu_L + \mu_R \neq 0$. The reason is simple: inhomogeneous quench does not excite any imbalance of vacancy momentum, which is a conserved quantity. However, in the perturbative linear-potential quench derivation of linear response coefficients (Sec. A of the Supplemental Material [33]) one has a natural vacancy momentum bias which generates the Drude weight.

Discussion.—We have studied transport properties of a simple reversible and deterministic cellular automaton. Despite its simplicity the model exhibits a large variety of transport phenomena, including charge diffusion, and offers an analytical handle on the calculation of transport coefficients, as well as exactly solving interesting initial value problems. The algebraic structure of the model

enables the identification of microscopic mechanisms behind its various transport regimes. Specifically, the ballistic behavior of certain degrees of freedom can induce the diffusive transport of charge carriers, which are completely frozen in their absence.

Our results open many interesting questions. First, it should be clarified whether the many body deterministic diffusion mechanism disclosed here applies to other integrable models, in particular to quantum lattice models such as XXZ, or to the quantized version of the hereby presented model. A promising idea in this direction is a formulation of quantum transport in terms of a classical-like soliton gas [11]. Second, our exactly solvable model could serve as a test bed for a precise verification of predictions of GHD. And third, one may imagine various solvable generalizations of our model. For example, we can define a stochastic Markov chain model by introducing a tunneling probability Γ for a particle exchange, i.e., to modify the following matrix elements of the local propagator $U_{(\pm,\mp),(\mp,\pm)} = \Gamma$, $U_{(\pm,\mp),(\pm,\mp)} = 1-\Gamma \equiv \bar{\Gamma}$. Our analysis can be straightforwardly extended, resulting in the same value of the Drude weight as for the deterministic case $\Gamma = 0$, while the Green-Kubo diffusion constant has a continuous dependence on Γ

$$\mathcal{D} = \frac{\Gamma^2 + \bar{\Gamma}(1-\bar{\Gamma}\rho)(\Gamma(\bar{\rho}^2 - \Gamma\rho(\rho+1)) + \bar{\rho})}{\bar{\Gamma}\rho(1-\bar{\Gamma}\rho)} \qquad (25)$$

and diverges at $\Gamma = 1$. This implies that the physics of our model is robust against adding a small noise or dissipation.

We acknowledge fruitful discussions with Bruno Bertini, Enej Ilievski, Spyros Sotiriadis, Lenart Zadnik, and Marko Žnidarič, and Herbert Spohn for useful comments. The work has been supported by Grants No. P1-0044 and No. N1-0025 of Slovenian Research Agency, and ERC Grant OMNES.

[1] H. Spohn, *Large Scale Dynamics of Interacting Particles* (Springer Science & Business Media, New York, 2012).
[2] D. Bernard and B. Doyon, J. Stat. Mech. (2016) 064005.
[3] O. A. Castro-Alvaredo, B. Doyon, and T. Yoshimura, Phys. Rev. X **6**, 041065 (2016).
[4] B. Bertini, M. Collura, J. De Nardis, and M. Fagotti, Phys. Rev. Lett. **117**, 207201 (2016).
[5] S. Sotiriadis, arXiv:1612.00373.
[6] A. De Luca, M. Collura, and J. De Nardis, Phys. Rev. B **96**, 020403 (2017).
[7] E. Ilievski and J. De Nardis, Phys. Rev. Lett. **119**, 020602 (2017).
[8] V. B. Bulchandani, R. Vasseur, C. Karrasch, and J. E. Moore, arXiv:1702.06146 [Phys. Rev. B (to be published)].
[9] B. Doyon and H. Spohn, arXiv:1703.05971.
[10] B. Doyon, H. Spohn, and T. Yoshimura, arXiv:1704.04409.
[11] B. Doyon, T. Yoshimura, and J.-S. Caux, arXiv:1704.05482.
[12] T. Prosen, Phys. Rev. E **89**, 012142 (2014).
[13] M. Medenjak, C. Karrasch, and T. Prosen, Phys. Rev. Lett. **119**, 080602 (2017).
[14] L. Bonnes, F. H. Essler, and A. M. Läuchli, Phys. Rev. Lett. **113**, 187203 (2014).
[15] M. Ljubotina, M. Znidaric, and T. Prosen, Nat. Commun. **8**, 16117 (2017).
[16] T. Prosen and M. Žnidarič, J. Stat. Mech. (2009) P02035.
[17] R. Steinigeweg and W. Brenig, Phys. Rev. Lett. **107**, 250602 (2011).
[18] R. Steinigeweg, Phys. Rev. E **84**, 011136 (2011).
[19] R. Steinigeweg, J. Gemmer, and W. Brenig, Phys. Rev. Lett. **112**, 120601 (2014).
[20] C. Karrasch, J. E. Moore, and F. Heidrich-Meisner, Phys. Rev. B **89**, 075139 (2014).
[21] H. Spohn and J. L. Lebowitz, Commun. Math. Phys. **54**, 97 (1977).
[22] A. Bobenko, M. Bordemann, C. Gunn, and U. Pinkall, Commun. Math. Phys. **158**, 127 (1993).
[23] T. Tokihiro, D. Takahashi, J. Matsukidaira, and J. Satsuma, Phys. Rev. Lett. **76**, 3247 (1996).
[24] T. Prosen and C. Meja-Monasterio, J. Phys. A **49**, 185003 (2016).
[25] T. Prosen and B. Buča, arXiv:1705.06645.
[26] In this sense our model belongs to a class of hard-rod systems [27–31]. However, considering particle positions to take values on the lattice $\mathbb{Z}$ rather than on the line $\mathbb{R}$ has two conceptual advantages: (i) The information (entropy) density in the initial condition is qualitatively smaller and diffusion cannot be attributed to random phases with which different particles collide even if velocities have a discrete distribution. (ii) Dynamics can be analyzed in terms of simple linear algebra and matrix spectral problems.
[27] D. Jepsen, J. Math. Phys. **6**, 405 (1965).
[28] J. Lebowitz, J. Percus, and J. Sykes, Phys. Rev. **171**, 224 (1968).
[29] J. Lebowitz, J. Percus, and J. Sykes, Phys. Rev. **188**, 487 (1969).
[30] D. Dürr, S. Goldstein, and J. L. Lebowitz, Commun. Pure Applied Math. **38**, 573 (1985).
[31] V. Balakrishnan, I. Bena, and C. Van den Broeck, Phys. Rev. E **65**, 031102 (2002).
[32] Note that in the canonical basis $[\alpha_1, \ldots, \alpha_n]$, U is a permutation matrix given in terms of local propagators $(U_{x,y})_{\underline{s}',\underline{s}} = \delta_{\underline{s}',\phi_{x,y}(\underline{s})}$.
[33] See Supplemental Material at http://link.aps.org/supplemental/10.1103/PhysRevLett.119.110603 for the derivation of the linear response coefficients, the details on the calculations of autocorrelation functions, steady state profiles and Monte Carlo simulation.
[34] E. Ilievski and T. Prosen, Commun. Math. Phys. **318**, 809 (2013).
[35] H. Spohn, arXiv:1707.02159.